Pseudo-spin-gap and slow spin fluctuation in $La_{2-x}Sr_xCuO_4$ ($x=0.13$ and 0.18) via ^{63}Cu and ^{139}La nuclear quadrupole resonance

Y. Itoh,[1,2] T. Machi,[1] N. Koshizuka,[1] M. Murakami,[1] H. Yamagata,[3] and M. Matsumura[3]
[1]*Superconductivity Research Laboratory, International Superconductivity Technology Center, 1-10-13 Shinonome, Koto-ku Tokyo 135-0062, Japan*
[2]*Japan Society for the Promotion of Science, Tokyo 102-8471, Japan*
[3]*Department of Material Science, Faculty of Science, Kochi University, Kochi 780-8520, Japan*
(Received 9 July 2003; revised manuscript received 23 February 2004; published 10 May 2004; publisher error corrected 12 May 2004)

We analyzed nonexponential ^{63}Cu nuclear spin-lattice relaxation curves for ^{63}Cu-enriched high-T_c superconductors: $La_{2-x}Sr_xCuO_4$ with $x=0.13$ (slightly underdoped) and 0.18 (slightly overdoped), and studied the applicability of an impurity-induced nuclear spin-lattice relaxation theory. We found a remnant of pseudo-spin-gap effect on the host ^{63}Cu nuclear spin-lattice relaxation time and slow inhomogeneous spin fluctuation via the impurity-induced relaxation time. The effect of slow spin dynamics was also observed in ^{139}La nuclear spin-lattice relaxation. The inhomogeneous electron-spin fluctuation, which is associated with randomly distributed staggered moments on the CuO_2 plane, smears the pseudo-spin-gap. The fact that the optimal $T_c \sim 38$ K is smaller than $T_c \sim 96$ K of $HgBa_2CuO_{4+\delta}$ can be attributed to the depairing effect due to the slow spin fluctuation.

DOI: 10.1103/PhysRevB.69.184503 PACS number(s): 76.60.−k, 74.25.Nf, 74.72.Bk

I. INTRODUCTION

Single-CuO_2-layer superconductors $La_{2-x}Sr_xCuO_4$ (LSCO, the optimal $T_c \sim 38$ K) had been thought to be a homogeneous electronic system. According to the superconductivity theory based on antiferromagnetic spin fluctuation,[1,2] a small spin-fluctuation energy $\hbar\Gamma$ is responsible for the fact that the optimal T_c of LSCO is lower than the other high T_c (~ 100 K) systems. However, the discovery of charge-spin stripe correlation through a neutron-diffraction technique renewed our understanding of the electric or magnetic states of LSCO.[3] A series of intensive nuclear-magnetic-resonance (NMR) and nuclear quadrupole resonance (NQR) studies revealed inhomogeneous electronic states both in static and dynamic response; widely distributed spin-fluctuation energy, segregated electronic phases, and the glassy nature of charge-spin stripe ordering.[4–20] Inelastic neutron-scattering experiments showed that dynamical spin susceptibility $\chi''(q,\omega)$ of the CuO_2 plane possesses a complicated structure at low frequencies and a broad tail at high frequencies over a hundred meV.[21]

Pseudo-spin-gap or pseudogap has been believed to be the key to understanding the mechanism of superconductivity.[22–25] The normal-state gap effect on LSCO is, however, still controversial. A similar magnitude of pseudogap in the electronic density of states (~ 30 meV) is observed in photoemission spectra both for single-layer superconductors, LSCO with the optimal $T_c \sim 38$ K (Ref. 26), and $HgBa_2CuO_{4-\delta}$ (Hg1201, the optimal $T_c \sim 96$ K) (Ref. 27). In contrast, the pseudo-spin-gap effect on low-energy magnetic excitation, which is measured from Cu nuclear spin-lattice relaxation rate $1/T_1$,[28] is different between LSCO (Refs. 20 and 29) and Hg1201 (Refs. 30 and 31). The pseudo-spin-gap effect on $1/T_1T$ (T is temperature) is seen as the normal-state depression of $1/T_1T$ above T_c.[22] For Hg1201, the pseudo-spin-gap temperature T_s, at which $1/T_1T$ starts to decrease, is ~ 260 K for underdoped samples ($T_c \sim 50$ K) and ~ 140 K for optimal and overdoped samples ($T_c \sim 96$–30 K). The signature of LSCO is, however, observed only just above T_c, i.e., $T_s \sim 45$–50 K around the optimally doped level.[20,29] The above-T_c pseudo-spin-gap effect on $\chi''(q,\omega)$, which is measured with an inelastic neutron-scattering technique, seems to be different between the double-CuO_2-layer $YBa_2Cu_3O_{7-\delta}$ (Y123 or YBCO) Refs. 32 and 33 and the single-layer LSCO (Refs. 34 and 35). There is no report on the neutron scattering for Hg1201.

Slow spin fluctuation with a frequency $\nu_{slow}(<k_BT/h)$ causes the depairing effect.[1,36–38]. The wipeout effect on NMR/NQR spectrum, which indicates the existence of slow fluctuation and an inhomogeneous electronic state, is observed in lightly doped LSCO (Refs. 8 and 39) as well as Zn-substituted YBCO (Ref. 40). Some phase fluctuation effect will alter the electronic state over the whole doped regions.[41] Here we address the question of whether the slow, inhomogeneous spin fluctuation smears the pseudo-spin-gap or whether the magnetic excitation spectrum of LSCO is gapless. This question has long been sought by several authors.[24,42,43]

Nonexponential relaxation is commonly observed in disordered or inhomogeneous materials.[44] For LSCO, the nonexponential relaxation is observed in planar Cu nuclear spin-lattice relaxation curves[11,45,46] such as in-plane impurity-doped Y123.[47] The magnetic impurity-induced NMR relaxation theory,[48] which is based on the slow spin fluctuation and the wipeout effect, has successfully accounted for the nonexponential recovery curves in the impurity-doped YBCO.[49–51] However, to our knowledge, no one has ever applied this model to the superconducting LSCO at around the optimally doped level. Diffraction techniques (neutron or x-ray scatterings) are suitable for detecting a coherent motion well defined by specific wave vectors in momentum space, whereas a NMR/NQR technique is suited to detect an incoherent motion such as local magnetic or electric density os-

cillations in real space. Hence, the detailed analyses on the relaxation curves will help us to clarify the magnetic correlation in real space, which cannot easily be deduced either by diffraction methods or scanning tunneling spectroscopy.

In this paper, we measured Cu NQR nuclear spin-lattice relaxation of ^{63}Cu-enriched LSCO with $x=0.13$ (slightly underdoped) and 0.18 (slightly overdoped) (Ref. 20) and studied the applicability of an impurity-induced NMR relaxation theory to LSCO. The ^{63}Cu isotope enrichment is useful for performing precise measurements in LSCO, which was first demonstrated in our previous report[20] and later confirmed in Refs. 8–11. In a model with randomly distributed impurity relaxation centers, a remnant of the pseudo-spin-gap affects the host Cu nuclear spin-lattice relaxation rate; and slow, inhomogeneous spin dynamics affect the impurity-induced Cu NQR relaxation rate. Incoherent spin fluctuation, which is a spatially inhomogeneous relaxation process, smears the pseudo-spin-gap effect on the low frequency spin dynamics. We also found similar effects on ^{139}La nuclear spin-lattice relaxation curves and the time constant $^{139}T_1$. ^{139}La NQR can provide information on short $^{63}T_1$ signals in Cu NQR spectrum, which was confirmed in Refs. 5,9,15–17. It can interpolate ^{63}Cu NQR and muon spin relaxation. In general, the nuclear spin-lattice relaxation time T_1 is expressed by an electron-spin-fluctuation time τ_e,

$$1/T_1 = A^2 \frac{\tau_e}{1+(2\pi\nu_{res}\tau_e)^2}, \tag{1}$$

where A is a nuclear-electron coupling constant and ν_{res} is a nuclear resonance frequency. This is based on the Bloembergen-Purcell-Pound model.[52] Compared to the ^{63}Cu nuclear moment, ^{139}La nuclear moment is a better probe for detecting slow spin fluctuation on the CuO_2 plane due to a weak electron-nuclear coupling, $^{139}(1/T_1)/^{63}(1/T_1)\sim 0.4\times 10^{-4}$.[9]

II. EXPERIMENT

The powder samples employed in the present study are identical to those used in the previous study.[20] The powders were mixed with Stycast 1266 epoxy and magnetically aligned along the c axis. The superconducting transition temperatures were measured with a superconducting quantum interference device (SQUID) magnetometer, and T_c values were ~ 36 K for $x=0.13$ and $T_c\sim 34$ K for $x=0.18$ in the presence of $H=100$ Oe. The normal-state uniform magnetic susceptibility in $H=1$ T measured with a SQUID magnetometer was similar to that reported in Ref. 53. No Curie term was observed.

A phase-coherent-type pulsed spectrometer was utilized to perform ^{63}Cu and ^{139}La NQR experiments. A spin-echo $\pi/2$-π pulse sequence ($\pi/2$-τ-π echo) was used to observe the signal. The zero-field ^{63}Cu and ^{139}La NQR frequency spectra with quadruple detection were obtained by integration of ^{63}Cu and ^{139}La nuclear spin echoes while changing the frequency. A typical width of the first exciting $\pi/2$-pulse t_w was about 3 μs (the excited frequency region $\nu_1 \sim 83$ kHz from $2\pi\nu_1 t_w=\pi/2$). Nuclear spin-lattice relaxation curves $p(t)\equiv 1-M(t)/M(\infty)$ (recovery curves) were measured by using an inversion recovery technique as functions of time t after an inversion pulse, where the nuclear spin-echo amplitude $M(t)$, $M(\infty)[\equiv M(10T_1)]$, and t were recorded.

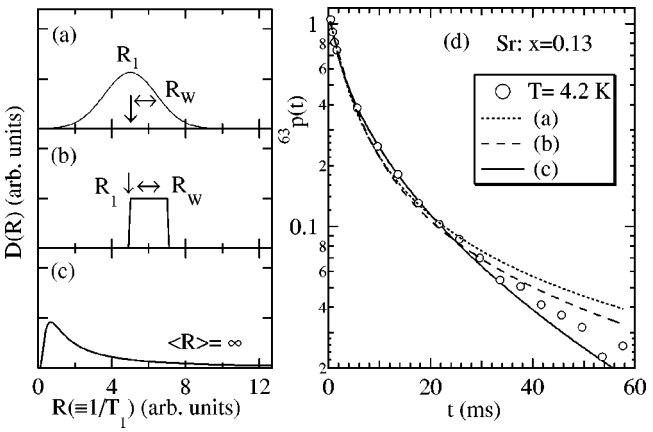

FIG. 1. Toy models of distribution function $D(R)$ with respect to $R\equiv 1/T_1$ (left); (a) a Gaussian distribution, (b) a rectangular distribution, and (c) a heavy-tailed distribution leading to a stretched exponential time function. (d) ^{63}Cu nuclear spin-lattice relaxation curve $p(t)$ (open circles) for Sr content of $x=0.13$ at $T=4.2$ K. The dotted, dashed, and solid curves are the least-squares fitting results using the distribution functions in (a), (b), and (c), respectively.

The dependence of ^{63}Cu T_1 on the pulse interval time τ was reported to be $\Delta T_1\sim 10\%$ between $\tau=12$ and $=24$ μs.[11] ^{63}Cu recovery curves were measured at $\tau=12$–18 μs for $x=0.13$ and at $\tau=13$–15 μs for $x=0.18$. ^{139}La recovery curves were measured at $\tau=31$–35 μs for $x=0.13$ and at $\tau=28$–35 μs for $x=0.18$. No appreciable τ dependence was observed within our experimental accuracy. We thus believe that the above change in τ leaves our conclusions unchanged.

III. RESULTS AND DISCUSSION

A. ^{63}Cu NQR

1. Nonexponential Cu nuclear spin-lattice relaxation curve

When the nuclear spin-lattice relaxation time T_1 follows a distribution function $D(R)(R\equiv 1/T_1)$, the nuclear spin-lattice relaxation curve $p(t)$ is expressed by

$$p(t)=p(0)\int_0^\infty dRD(R)\exp(-Rt) \tag{2}$$

with

$$\int_0^\infty dRD(R)=1. \tag{3}$$

Here we assume narrow, broad, and heavy-tailed distribution functions for T_1. Figures 1(a)–1(c) show three types of $D(R)$: (a) a Gaussian distribution of

$$D(R)=\sqrt{\frac{2}{\pi}}\frac{1}{R_W}\exp\left(-\frac{1}{2}\frac{(R-R_1)^2}{R_W^2}\right), \tag{4}$$

(b) a rectangular distribution of

$$D(R)=\begin{cases}1/R_W & R_1\leqslant R\leqslant R_1+R_W\\ 0 & R<R_1, R_1+R_W<R,\end{cases} \tag{5}$$

and (c) a heavy-tailed distribution, leading to a stretched exponential time function, of

$$D(R)=\frac{\sqrt{R_W}}{2\sqrt{\pi}R^{3/2}}\exp\left(-\frac{R_W}{4R}\right). \tag{6}$$

Here, we define $1/T_1\equiv R_1$ and $1/\tau_1\equiv R_W$.

Substituting Eqs. (4)–(6) into Eq. (2), we obtain the analytical expressions of

$$p(t)=p(0)e^{-R_1t-(R_Wt)^2}\mathrm{erfc}\left(R_Wt-\frac{R_1}{2R_W}\right)\Big/\ \mathrm{erfc}\left(-\frac{R_1}{2R_W}\right) \tag{7}$$

for the Gaussian distribution of Eq. (4) [(a)],

$$p(t)=p(0)e^{-R_1t}(1-e^{-R_Wt})/R_Wt \tag{8}$$

for the rectanglar distribution of Eq. (5) [(b)], and

$$p(t)=p(0)e^{-R_1t-\sqrt{R_Wt}} \tag{9}$$

for the heavy-tailed distribution of Eq. (6) [(c)]. In the case of Eq. (9), $p(0)$ in Eq. (2) is replaced by $p(0)e^{-R_1t}$ to involve a central uniform relaxation process.[54]

All the distribution functions of Eqs. (4)–(6) and the time developments of Eqs. (7)–(9) include the two time constants of T_1 and τ_1. The distribution functions of Eqs. (4) and (5) are characterized by finite moments of

$$\langle R^n\rangle=\int_0^\infty dRR^nD(R)\quad (n=1,2,\ldots). \tag{10}$$

On the other hand, the first moment $\langle R\rangle$ of Eq. (6) takes an infinite value. Therefore, the heavy-tailed distribution of Eq. (6) may be called *Lévy flights*.[55] Then, the time development expression of $p(t)$ of Eq. (9) is more convenient than the distribution function of Eq. (6). The analysis based on the distribution function $D(R)$ is more convenient for a narrow distribution around a central value R_1, that is, $R_W<R_1$. In the patch model for carrier distribution in a broad Cu NQR spectrum of LSCO,[11] low-temperature deviation from a single exponential function is attributed to an overlapping effect of the frequencies neighboring T_1. Some distribution functions can be introduced to account for a small deviation of the recovery curve from a single exponential function. For a large deviation, however, we will employ another model of Eq. (9). Figure 1(d) shows ^{63}Cu nuclear spin-lattice relaxation curve $p(t)$ (open circles) for the sample with Sr content of $x=0.13$ at $T=4.2$ K at a peak frequency of $\nu_{res}=35.5$ MHz. The dotted, dashed, and solid curves are the least-squares fitting results using Eqs. (7)–(9) with the distribution functions in (a), (b), and (c), respectively. The fitting parameters are $p(0)$, R_1, and R_W.

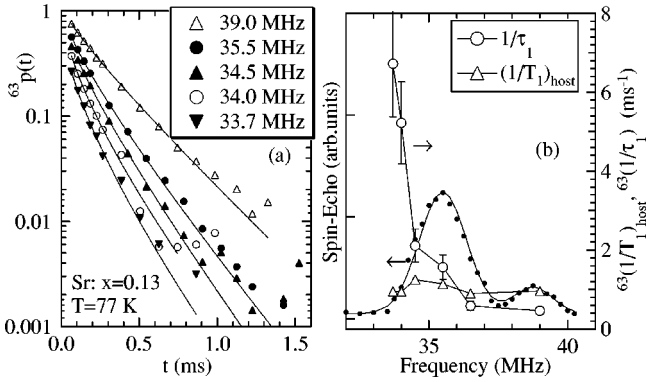

FIG. 2. (a) Frequency dependence of ^{63}Cu nuclear spin-lattice relaxation curve $^{63}p(t)$ in a broad ^{63}Cu NQR spectrum for Sr content of $x=0.13$ at $T=77$ K. The solid curves are the least-squares fitting results using Eq. (9) with fitting parameters $^{63}(\tau_1)$ and $^{63}(T_1)_{host}$. (b) The ^{63}Cu NQR frequency spectrum for Sr content of $x=0.13$ at $T=77$ K and the estimated relaxation rates $^{63}(1/\tau_1)$ and $^{63}(1/T_1)_{host}$ at the respective frequencies. The main Cu NQR spectrum around 35.5 MHz is called *A* line. The small spectrum around 39 MHz is called *B* line.

The best fitting result was obtained with Eq. (9) of the stretched exponential function. Equation (9) implies two relaxation processes: R_W due to some ''impurity'' relaxation centers randomly distributed on the CuO_2 plane; and R_1 due to the host Cu (homogeneous) electron-spin fluctuations.[48] Hereafter we call R_W in Eq. (9) an impurity-induced relaxation rate. Since no Curie term is observed in the uniform spin susceptibility, the ''impurity'' moment is not due to an external paramagnetic impurity in the CuO_2 plane. Randomly distributed staggered moments are assumed as in Refs. 17, 43, and 56.

2. Frequency-distributed Cu nuclear spin-lattice relaxation

Figure 2(a) shows the frequency dependence of the ^{63}Cu nuclear spin-lattice relaxation $^{63}p(t)$ across the inhomogeneously broadened ^{63}Cu NQR frequency spectrum for the sample with Sr content of $x=0.13$ at $T=77$ K. The strongly frequency dependent $^{63}p(t)$ was first reported in Ref. 7. The solid curves are the least-squares fitting results using Eq. (9). The fitting is reasonably good. Figure 2(b) shows the ^{63}Cu NQR spectrum, and the estimated $^{63}(1/T_1)_{host}(\equiv R_1/3)$ and $^{63}(1/\tau_1)(\equiv R_W/3)$ as a function of frequency ν_{res}. The numerical factor of 3 was employed to conform to a conventional definition of T_1.[28] Figure 2(b) demonstrates that a strong frequency dependence of the recovery curve results from $^{63}(1/\tau_1)$ but not $^{63}(1/T_1)_{host}$. This is a significant consequence from the analysis using Eq. (9).

3. Two models

One may infer two models to account for the frequency-distributed relaxation in a broad ^{63}Cu NQR spectrum. Figure 3 illustrates two models: (a) a ''patch'' model; and (b) a charge-density oscillation model. In the patch model (a) for

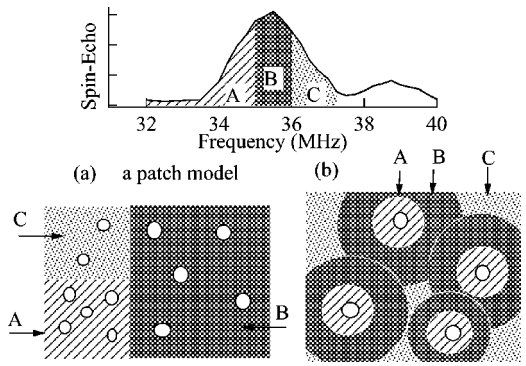

FIG. 3. Schematic ^{63}Cu NQR spectrum and top views of CuO_2 plane (a) and (b). We tentatively divide the frequency spectrum into *A*, *B*, and *C* regions. The hatched, shaded, dotted areas are assigned to the respective Cu NQR frequency regions. The small open circles are impurity relaxation centers. Figure (a) illustrates the impurity relaxation centers in the ''patch'' model. The lower-frequency regions correspond to the poorer hole concentration regions, and thereby more impurity relaxation centers or more enhanced relaxation centers. Figure (b) illustrates the impurity relaxation centers in a charge-density oscillation model.

the inhomogeneous hole distribution,[8–11] a lower-frequency side of the ^{63}Cu NQR spectrum represents a smaller hole-doped region. Since the in-plane impurity effect is more evident for less hole-doped YBCO (Ref. 51) and LSCO (Ref. 57), one can expect that the ''impurity'' relaxation centers enhance an impurity-induced relaxation rate $^{63}(1/\tau_1)$ via *A* and τ_e in Eq. (1) in a lower-frequency side more effectively than in a higher-frequency side. The other model (b) is for randomly distributed impurity relaxation centers and represents their induced charge density oscillations on the homogeneous hole distribution. The lower frequency side of the ^{63}Cu NQR spectrum is assigned to a region closer to the ''impurity'' relaxation centers that are associated with the staggered moments. In this context, this model is consistent with that proposed in Ref. 18 and similar to that for the Zn neighbor Cu NQR in YBCO (Ref. 51).

4. Temperature dependence of $^{63}(1/\tau_1)$: impurity-induced relaxation

The temperature dependence of the Cu recovery curve was also analyzed at representative frequencies for the samples with $x=0.13$ and 0.18 by using Eq. (9). The host Cu nuclear spin-lattice relaxation rate $^{63}(1/T_1)_{host}$ and the impurity-induced $^{63}(1/\tau_1)$ were estimated as a function of temperature. Figure 4 shows the plot of $^{63}(1/\tau_1)$ as a function of temperature at (a) a lower frequency of the *A* line, (b) the peak frequency of the *A* line, and (c) the peak frequency of the *B* line.

First, all the $^{63}(1/\tau_1)$ curves show peak behavior above T_c. A similar temperature dependence of $^{63}(1/\tau_1)$ for Zn substituted Y123 has been analyzed based on the Bloembergen-Purcell-Pound model of Eq. (1).[58] We thus analyzed $^{63}(1/\tau_1)$ of LSCO with this model, which approximates a part of the low-frequency dynamical spin susceptibility $\chi''(q,\omega)$. For lightly doped LSCO, the peak behavior

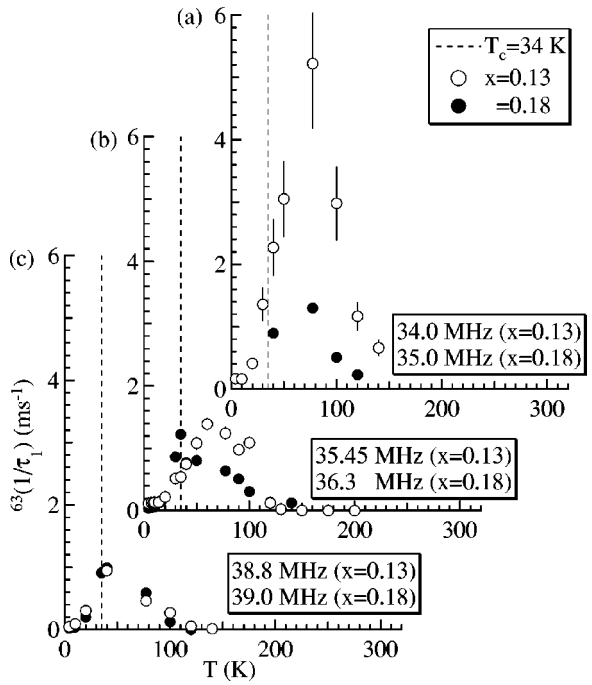

FIG. 4. Temperature dependence of $^{63}(1/\tau_1)$ in a broad Cu NQR spectrum: (a) a lower frequency of the *A* line, (b) the peak frequency of the *A* line, and (c) the peak frequency of the *B* line.

of the stretched exponential relaxation rate of ^{139}La nuclear spin-lattice relaxation is explained by an electron correlation time τ_e,

$$\tau_e(T)=\tau_e(\infty)e^{J_{eff}/T}, \tag{11}$$

where J_{eff} is an energy scale of the slow electron-spin-fluctuation spectrum, e.g., the spin freezing effect in two dimensional renormalized classical regime.[9,12,13] When $\tau_e(T)$ for $x=0.13$ and 0.18 increases with decreasing temperature, the peak is observed in $^{63}(1/\tau_1)$ at $\tau_e(T)=1/2\pi^{63}\nu_{res}$.

Second, the peak temperature T_{peak} is slightly dependent on the frequency, i.e., T_{peak} decreases from $\sim$77 K to $\sim$40 K with increasing frequency both for the samples with $x=0.13$ and 0.18. This is not explained in the frame of the above uniform Bloembergen-Purcell-Pound model, where T_{peak} should move to a higher value at high frequencies. A nonuniform Bloembergen-Purcell-Pound model must then be introduced.

If one assumes that both $\tau_e(\infty,\nu_{res})$ and $J_{eff}(\nu_{res})$ in Eq. (11) increase with decreasing ν_{res}, the frequency dependence of the peak temperature T_{peak} will be reproduced. The ''impurity'' spin correlation time $\tau_e(T,\nu_{res})$ is distributed in a broad ^{63}Cu NQR spectrum. The lower-frequency region in the broad Cu NQR spectrum, i.e., the hole-poor region in the patch model,[8,9] must exhibit slow spin fluctuation. Thus, the frequency dependence of the peak temperature T_{peak} is consistent with the patch model for the hole distribution. However, we do not discard the charge-density oscillation model with the staggered moments for the inhomogeneous hole distribution.

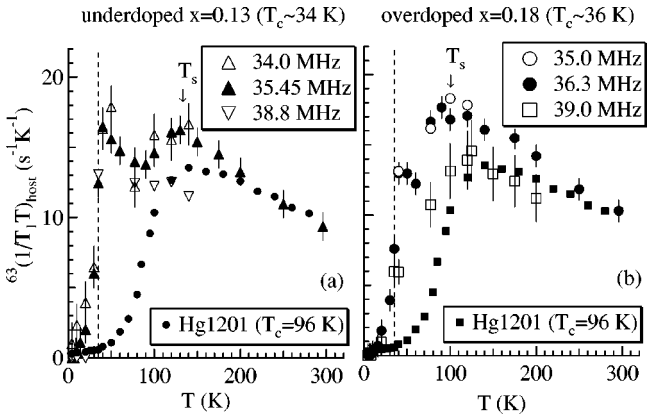

FIG. 5. Temperature dependence of the host ^{63}Cu nuclear spin-lattice relaxation rate $^{63}(1/T_1T)_{host}$ for (a) $x=0.13$ and (b) $x=0.18$. For reference, $^{63}(1/T_1T)$ of the optimally doped Hg1201 ($T_c=96$ K) is also shown in the figure. The pseudo-spin-gap behavior is seen at $T_s\sim 130$ K for $x=0.13$ and at ~ 90 K for $x=0.18$.

Third, the frequency dependence of $^{63}(1/\tau_1)$ is more remarkable for the sample with $x=0.13$ than for $x=0.18$. This is consistent with the fact that the frequency dependence of $^{63}\tau_1$ is more remarkable in less doped YBCO.[51] Thus, the temperature dependence (below about 150 K) of the inhomogeneous electronic state in Ref. 11 can be attributed to the impurity-induced relaxation on the inhomogeneous hole distribution.

5. Temperature dependence of $^{63}(1/T_1T)_{host}$: pseudo-spin-gap in host magnetic excitation

Figure 5 shows the plot of $^{63}(1/T_1T)_{host}$ as a function of temperature for (a) $x=0.13$ and (b) 0.18. For reference, $^{63}(1/T_1T)$ of Hg1201 with $T_c=96$ K is also plotted in the figure.[30] It is notable that the pseudo-spin-gap is clearly observed in $^{63}(1/T_1T)_{host}$.

With lowering temperature, $^{63}(1/T_1T)_{host}$ increases due to antiferromagnetic spin fluctuation and takes a maximum value at a pseudo-spin-gap temperature $T_s\sim 130$ K for $x=0.13$ and ~ 90 K for $x=0.18$. Unfortunately, the frequency dependence of T_s in the Cu NQR spectrum is not obvious with accuracy of our experiment. As the temperature is further decreased, $^{63}(1/T_1T)_{host}$ takes a minimum at $T_{min}\sim 90$ K for $x=0.13$ and at ~ 60 K for $x=0.18$; and thereafter increases again down to T_c. Below T_c, $^{63}(1/T_1T)_{host}$ rapidly decreases due to the opening of the superconducting gap. The upturn of $^{63}(1/T_1T)_{host}$ below T_{min} suggests the presence of a gapless mode in a homogeneous magnetic excitation. Its origin is not clear but it surely smears the pseudo-spin-gap.

B. ^{139}La NQR

1. ^{139}La nuclear spin-lattice relaxation curves

The ^{139}La nuclear spin-lattice relaxation curves were measured at the peak frequencies of the highest transition lines ($I_z=\pm 7/2\leftrightarrow\pm 5/2$ of nuclear spin $I=7/2$) of ^{139}La NQR spectra for $x=0.13$ and 0.18.[59,60]

Several functions for the analysis of the experimental recovery curves of ^{139}La NQR ($I=7/2$) are proposed.[9,17,61] To conform to the above analysis of ^{63}Cu NQR recovery curve, we analyzed the ^{139}La NQR recovery curve as follows. Equation (9) for the ^{63}Cu recovery curve $^{63}p(t)$ is rewritten by

$$^{63}p(t)=p(0)\begin{cases} e^{-\sqrt{R_W t}}, & t\ll R_W/R_1^2 \\ e^{-R_1 t}, & t\gg R_W/R_1^2. \end{cases} \tag{12}$$

On this analogy, we analyzed the ^{139}La NQR recovery curve $^{139}p(t)$ at the highest-frequency transition line ($I_z=7/2\leftrightarrow 5/2$) by

$$^{139}p(t)=p(0)\begin{cases} e^{-\sqrt{R_W t}}, & R_W t<1 \\ \dfrac{3}{7}e^{-3R_1 t}+\dfrac{100}{77}e^{-10R_1 t}+\dfrac{3}{11}e^{-21R_1 t}, & 21R_1 t>1. \end{cases} \tag{13}$$

The stretched exponential function of $^{139}p(t)$ originates from the mechanism similar to that of $^{63}p(t)$. The multiexponential recovery curve of Eq. (13) is a theoretical solution to the rate equations with homogeneous, single magnetic relaxation.[9,62]

Figure 6 shows ^{139}La NQR recovery curves $^{139}p(t)$ at the peak frequency of 18.33 MHz for $x=0.18$. The solid and the dashed curves are the respective least-squares fitting results using the stretched exponential and the multiexponential functions of Eq. (13). Logarithmic $p(t)$ versus t plots are for the recovery curves in longer t, and $p(t)$ versus logarithmic t plots are for those in shorter t. In Fig. 6, the dashed curves in the left panel are the fitting results for the data in $t<2$ s, whereas that in the right panel is the fitting curve in $t>2$ s. It should thus be noted that the dashed curves in the left and the right panels are different. The solid curves are not plotted in the right panel of Fig. 6.

At low temperatures below T_c, the stretched exponential function is a better fit to $^{139}p(t)$ in shorter t, rather than the multiexponential function. In contrast, the multiexponential function well fit $^{139}p(t)$ in the whole t range above T_c. Thus, the slow, inhomogeneous spin fluctuation also affects

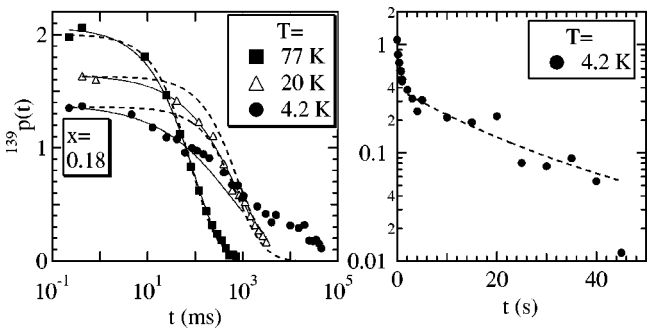

FIG. 6. ^{139}La nuclear-spin-lattice relaxation curves $^{139}p(t)$ for Sr content of $x=0.18$ at $T=4.2$ K, 20 K and 77 K; $p(t)$ vs logarithmic t plots (left) and logarithmic $p(t)$ vs t plots (right). The solid and the dashed curves are the least-squares fitting results using the stretched exponential and the multiexponential functions of Eq. (13), respectively. The stretched exponential functions (solid curves) are not plotted in the right panel. The dashed curves in the left panel are the fitting results for $t<2$ s, whereas that in the right panel is for $t>2$ s.

the low temperature ^{139}La nuclear spin-lattice relaxation. We could not confirm the frequency dependence of $^{139}p(t)$ in the broad ^{139}La NQR spectra.

2. $^{139}\tau_1$ and $^{139}(T_1)$

Figure 7 shows the plot of $^{139}(1/\tau_1)(\equiv R_W)$ and $^{139}(1/T_1)(\equiv R_1)$ estimated by using Eq. (13). For comparison, the $^{139}(1/\tau_1)$ of lightly doped, nonsuperconducting LSCO with $x=0.018$ is also plotted using the data reported in Ref. 13.

Below T_c, $^{139}(1/T_1)$ rapidly decreases due to opening of the superconducting gap, which is consistent with the ^{63}Cu NQR results. The magnitude of $^{139}(1/\tau_1)$ decreases from $x=0.018$ to 0.13 and further to 0.18, being qualitatively in agreement with the previous observations.[5,61] For $x=0.13$, $^{139}(1/\tau_1)$ moderately increases with decreasing temperature, while for $x=0.18$ it is nearly independent of temperature.

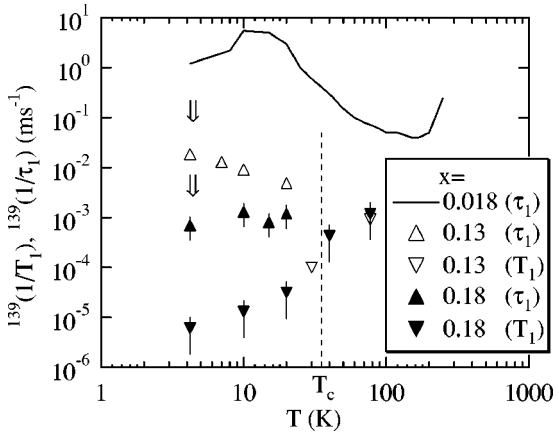

FIG. 7. Temperature dependence of ^{139}La nuclear spin-lattice relaxation rates $^{139}(1/\tau_1)$ and $^{139}(1/T_1)_{host}$ for $x=0.13$ and 0.18. For reference, $^{139}(1/\tau_1)$ of lightly doped, nonsuperconductor LSCO with $x=0.018$ is reproduced from Ref. 13. The arrow (⇓) indicates the direction of change with Sr doping.

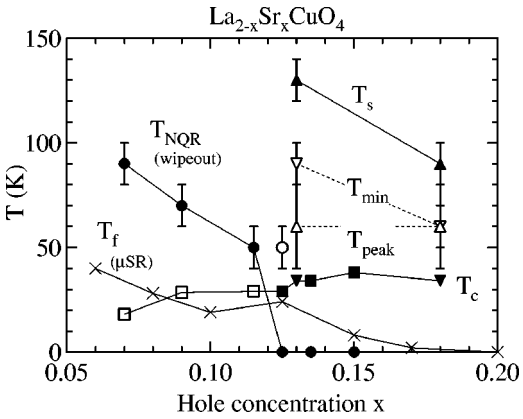

FIG. 8. Magnetic phase diagram of LSCO with the pseudo-spin-gap effect constructed based on the data in the present work and the wipeout effect in Ref. 8. The characteristic temperatures against the Sr content x or hole concentration. T_c (squares) and the Cu NQR wipeout temperatures T_{NQR} (circles) are reproduced from Ref. 8. The crossover temperatures T_f (crosses), which is the onset of deviation of muon spin relaxation from Gaussian behavior, are reproduced from Ref. 63. T_c, T_s, T_{min}, and T_{peak} (triangles) are defined in Figs. 4 and 5.

The low temperature increase of $^{139}(1/\tau_1)$ for $x=0.018$ is explained in terms of the spin freezing effect, which coexists with superconductivity for $0.06<x<0.125$.[12,13,15–17] The moderate increase of $^{139}(1/\tau_1)$ for $x=0.13$ may be a remnant of such a spin freezing effect.

The behavior of $^{139}(1/\tau_1)$ below T_c is different from that of $^{63}(1/\tau_1)$. One may regard the peak temperature of $^{139}(1/\tau_1)$ as $^{139}T_{peak}<4.2$ K. Since the ^{139}La NQR frequency $^{139}\nu_{res}$ is totally lower than the ^{63}Cu NQR frequency $^{63}\nu_{res}$, the spin fluctuation via the ^{139}La NQR is slower than that via the ^{63}Cu NQR. From $^{139}T_{peak}<4.2$ K $<{}^{63}T_{peak}$ ($\sim$77 K), we obtain $(2\pi^{139}\nu_{res})^{-1}>\tau_e(4.2\text{ K})$ and $(2\pi^{63}\nu_{res})^{-1}=\tau_e(T\sim 77\text{ K})$. If one assumes Eq. (11) for $x=0.13$ and 0.18, then $^{63}\nu_{res}=35$ MHz and $^{139}\nu_{res}=18$ MHz lead to $0<J_{eff}<2.9$ K. The small J_{eff} is consistent with the result in Ref. 12.

C. Magnetic phase diagram

Figure 8 is the magnetic phase diagram constructed on the basis of the experimental results obtained in the present and the previous studies.[8,63] T_c (squares) and the Cu NQR wipeout temperatures T_{NQR} (circles) are reproduced from Ref. 8. The crossover temperatures T_f (crosses), where the time dependence of zero-field muon spin asymmetry first deviates from Gaussian behavior due to the slow fluctuation, are reproduced from Ref. 63. The triangular symbols of T_c, T_s, T_{min}, and T_{peak} are for the data obtained in the present work.

The pseudo-spin-gap temperatures T_s of LSCO lie on the same order of magnitude as the other cuprates Hg1201 or YBCO. For $x<0.13$, according to Ref. 8, the slow, inhomogeneous fluctuation affects the Cu spin dynamics on the whole CuO_2 planes and induce a large wipeout effect on the Cu NQR spectrum below T_{NQR}. For $x\geqslant 0.13$, our results

indicate that the moderate slow, inhomogeneous fluctuation still exists and affects the nuclear spin-lattice relaxation around T_{peak} but induces no appreciable wipeout effect. At low temperatures, the fluctuation slows down sufficiently to enter the time scale of the muon probe and to yield a fast muon relaxation below T_f.[63] The slow fluctuation below T_{peak} smears the pseudo-spin-gap. The unknown, gapless mode below T_{min}, which also masks the pseudo-spin-gap, may be a remnant of charge-spin stripe fluctuation. The slow, inhomogeneous fluctuation at T_{peak} around the optimally doped region are the characteristics of the magnetic phase diagram of LSCO, which contrasts with those of Hg1201 and YBCO. Thus, one reason why the optimal T_c of LSCO is lower than those of Hg1201 and YBCO is attributable to the depairing effect of the slow, inhomogeneous fluctuation.

The recent inelastic neutron scattering measurements of $\chi''(q,\omega)$ of LSCO indicate a threshold energy gap $E_g \sim 4$ meV and a small peak at ~ 6 meV above T_c,[34] which are different from the pseudo-spin-gap effect on $\chi''(q,\omega)$ of Y123.[32] The impurity-induced relaxation theory is crucial in deducing the pseudo-spin-gap behavior from the original relaxation data. Since we assume that the impurity-induced relaxation of LSCO is similar to that of Zn substituted YBCO, the low temperature peak around 6 meV in LSCO (Ref. 34) will correspond to the in-gap state at the antiferromagnetic wave vector, around 6 or 9 meV in Zn-substituted Y123 (Refs. 64 and 65). The randomly distributed, slow staggered moments on the CuO_2 plane are theoretically proposed.[43,56,66,67]

IV. CONCLUSION

From the analyses of ^{63}Cu and ^{139}La nuclear spin-lattice relaxation curves for LSCO, we found a remnant of the pseudo-spin-gap effect, comparable to Hg1201, and a slow spin fluctuation effect. This slow spin-fluctuation originates from a remnant of the spin freezing effect or the wipeout effect, which is more remarkable in less doped samples. Randomly distributed staggered moments with slow fluctuation may be responsible for the fact that LSCO exhibits relatively lower T_c than Hg1201.

ACKNOWLEDGMENTS

This work was supported by the New Energy and Industrial Technology Development Organization (NEDO) as Collaborative Research and Development of Fundamental Technologies for Superconductivity Applications.

[1] T. Moriya and K. Ueda, Adv. Phys. **49**, 555 (2000); J. Phys. Soc. Jpn. **63**, 1871 (1994).
[2] D. Pines, Physica B **163**, 78 (1990).
[3] J.M. Tranquada, B.J. Sternlieb, J.D. Axe, Y. Nakamura, and S. Uchida, Nature (London) **375**, 561 (1995).
[4] K. Yoshimura, T. Imai, T. Shimizu, Y. Ueda, K. Kosuge, and H. Yasuoka, J. Phys. Soc. Jpn. **58**, 3057 (1989).
[5] K. Yoshimura, T. Uemura, M. Kato, T. Shibata, K. Kosuge, T. Imai, and H. Yasuoka, in *The Physics and Chemistry of Oxide Superconductors*, edited by Y. Iye and H. Yasuoka (Springer-Verlag, Berlin, 1992), p. 405.
[6] K. Yoshimura, T. Uemura, M. Kato, K. Kosuge, T. Imai, and H. Yasuoka, Hyperfine Interact. **79**, 867 (1993).
[7] S. Fujiyama, Y. Itoh, H. Yasuoka, and Y. Ueda, J. Phys. Soc. Jpn. **66**, 2864 (1997).
[8] A.W. Hunt, P.M. Singer, K.R. Thurber, and T. Imai, Phys. Rev. Lett. **82**, 4300 (1999).
[9] A.W. Hunt, P.M. Singer, A.F. Cederström, and T. Imai, Phys. Rev. B **64**, 134525 (2001).
[10] P.M. Singer, A.W. Hunt, and T. Imai, Phys. Rev. Lett. **88**, 047602 (2002).
[11] P.M. Singer, A.W. Hunt, and T. Imai, cond-mat/0302078 (unpublished).
[12] J.H. Cho, F. Borsa, D.C. Johnston, and D.R. Torgeson, Phys. Rev. B **46**, 3179 (1992).
[13] F.C. Chou, F. Borsa, J.H. Cho, D.C. Johnston, A. Lascialfari, D.R. Torgeson, and J. Ziolo, Phys. Rev. Lett. **71**, 2323 (1993).
[14] E. Kukovitsky, H. Luetgemeier, and G. Teitel'baum, Physica C **252**, 160 (1995).
[15] M.-H. Julien, F. Borsa, P. Carretta, M. Horvatić, C. Berthier, and C.T. Lin, Phys. Rev. Lett. **83**, 604 (1999).
[16] M.-H. Julien, P. Carretta, and F. Borsa, Appl. Magn. Reson. **19**, 287 (2000).
[17] M.-H. Julien, A. Campana, A. Rigamonti, P. Carretta, F. Borsa, P. Kuhns, A.P. Reyes, W.G. Moulton, M. Horvatić, C. Berthier, A. Vietkin, and A. Revcolevschi, Phys. Rev. B **63**, 144508 (2001).
[18] J. Haase, R. Stern, D. G. Hinks, and C. P. Slichter, in *Stripes and Related Phenomena*, edited by A. Bianconi and N. L. Saini, (Kluwer, Dordrecht, New York, 2000), p. 303; J. Haase, C.P. Slichter, R. Stern, C.T. Milling, and D.G. Hinks, Physica C **341-348**, 1727 (2000).
[19] Y. Itoh, M. Matsumura, H. Yamagata, and H. Miyamoto, J. Phys. Soc. Jpn. **65**, 695 (1996).
[20] Y. Itoh, M. Matsumura, and H. Yamagata, J. Phys. Soc. Jpn. **65**, 3747 (1996).
[21] Y. Endoh, T. Fukuda, S. Wakimoto, M. Arai, K. Yamada, and S.M. Bennington, J. Phys. Soc. Jpn. Suppl. B **69**, 16 (2000).
[22] H. Yasuoka, T. Imai, and T. Shimizu, in *Strong Correlation and Superconductivity*, edited by H. Fukuyama, S. Maekawa, and A. P. Malozemoff (Springer-Verlag, Berlin, 1989), p. 254.
[23] T.M. Rice, in *The Physics and Chemistry of Oxide Superconductors*, edited by Y. Iye and H. Yasuoka (Springer-Verlag, Berlin, 1992), p. 313.
[24] T. Tanamoto, H. Kohno, and H. Fukuyama, J. Phys. Soc. Jpn. **63**, 2739 (1994).
[25] C. Berthier, M.H. Julien, M. Horvatić, and Y. Berthier, J. Phys. I **6**, 2205 (1996).
[26] T. Sato, T. Yokoya, Y. Naitoh, T. Takahashi, K. Yamada, and Y. Endoh, Phys. Rev. Lett. **83**, 2254 (1999).
[27] H. Uchiyama, W.-Z. Hu, A. Yamamoto, S. Tajima, K. Saiki, and A. Koma, Phys. Rev. B **62**, 615 (2000).
[28] T. Moriya, Prog. Theor. Phys. **16**, 23 (1956); **16**, 641 (1956); **28**, 371 (1962).

[29] T. Imai, J. Phys. Soc. Jpn. **59**, 2508 (1990).
[30] Y. Itoh, T. Machi, A. Fukuoka, K. Tanabe, and H. Yasuoka, J. Phys. Soc. Jpn. **65**, 3751 (1996).
[31] Y. Itoh, T. Machi, S. Adachi, A. Fukuoka, K. Tanabe, and H. Yasuoka, J. Phys. Soc. Jpn. **67**, 312 (1998).
[32] J. Rossat-Mignot, L.P. Regnault, C. Vettier, P. Bourges, P. Burlet, J. Bossy, J.Y. Henry, and G. Lapertot, Physica C **185-189**, 86 (1991).
[33] J. Rossat-Mignot, L.P. Regnault, P. Bourges, C. Vettier, P. Burlet, and J.Y. Henry, Phys. Scr., T **45**, 74 (1992).
[34] C.H. Lee, K. Yamada, Y. Endoh, G. Shirane, R.J. Birgeneau, M.A. Kastner, M. Greven, and Y-J. Kim, J. Phys. Soc. Jpn. **69**, 1170 (2000).
[35] C.H. Lee, K. Yamada, H. Hiraka, C.R. Venkateswara Rao, and Y. Endoh, Phys. Rev. B **67**, 134521 (2003).
[36] A.J. Millis, S. Sachdev, and C.M. Varma, Phys. Rev. B **37**, 4975 (1988).
[37] Y. Ohashi and H. Shiba, J. Phys. Soc. Jpn. **62**, 2783 (1993).
[38] P. Monthoux and D.J. Scalapino, Phys. Rev. B **50**, 10339 (1994).
[39] T. Imai, K. Yoshimura, T. Uemura, H. Yasuoka, and K. Kosuge, J. Phys. Soc. Jpn. **59**, 3846 (1990).
[40] H. Yamagata, K. Inada, and M. Matsumura, Physica C **185-189**, 1101 (1991).
[41] K. Yoshimura, Y. Nishizawa, Y. Ueda, and K. Kosuge, J. Phys. Soc. Jpn. **59**, 3073 (1990).
[42] D. Pines, Physica C **341-348**, 59 (2000).
[43] A.J. Millis and H. Monien, Phys. Rev. Lett. **70**, 2810 (1993).
[44] H. Scher, M.F. Shlesinger, and J.T. Bendler, Phys. Today **41** {1}, 26 (1991).
[45] S. Ohsugi, Y. Kitaoka, K. Ishida, and K. Asayama, J. Phys. Soc. Jpn. **60**, 2351 (1991).
[46] S. Ohsugi, Y. Kitaoka, K. Ishida, G.-Q. Zheng, and K. Asayama, J. Phys. Soc. Jpn. **63**, 700 (1994).
[47] K. Ishida, Y. Kitaoka, N. Ogata, T. Kamino, K. Asayama, J.R. Cooper, and N. Athanassopoulou, J. Phys. Soc. Jpn. **62**, 2803 (1993).
[48] M.R. McHenry, B.G. Silbernagel, and J.H. Wernick, Phys. Rev. Lett. **27**, 426 (1971); Phys. Rev. B **5**, 2958 (1972).
[49] Y. Itoh, T. Machi, N. Watanabe, and N. Koshizuka, Physica C **357-360**, 69 (2001).
[50] Y. Itoh, T. Machi, N. Watanabe, and N. Koshizuka, J. Phys. Soc. Jpn. **70**, 644 (2001).
[51] Y. Itoh, T. Machi, C. Kasai, S. Adachi, N. Watanabe, N. Koshizuka, and M. Murakami, Phys. Rev. B **67**, 064516 (2003).
[52] N. Bloembergen, E.M. Purcell, and R.V. Pound, Phys. Rev. **73**, 679 (1948).
[53] L.F. Schneemeyer, J.V. Waszczak, E.A. Rietman, and R.J. Cava, Phys. Rev. B **35**, 8421 (1987).
[54] In passing, one may assume a function of

$$p(t)=p(0)\exp[-(R_1 t)^{\beta}]$$

with fitting parameters $p(0)$, R_1, and β. From the actual least-squares fit using this equation, we observed a decrease of β from 1 to 0.5 when cooled below 150 K, but nearly the same T dependence of R_1 as in Ref. 20. Thus, we do not study the above equation hereafter in the present study.
[55] J. Klafter, M.F. Shlesinger, and G. Zumofen, Phys. Today **49** {2), 33 (1996).
[56] Y. Ohashi, Phys. Rev. B **60**, 15388 (1999).
[57] H. Yamagata, H. Miyamoto, K. Nakamura, M. Matsumura, and Y. Itoh, J. Phys. Soc. Jpn. **72**, 1768 (2003).
[58] Y. Itoh, T. Machi, C. Kasai, S. Adachi, N. Watanabe, N. Koshizuka, and M. Murakami, Physica C **392-396**, 166 (2003).
[59] H. Nishihara, H. Yasuoka, T. Shimizu, T. Tsuda, T. Imai, S. Sasaki, S. Kanbe, K. Kishio, K. Kitazawa, and K. Fueki, J. Phys. Soc. Jpn. **56**, 4559 (1987).
[60] S. Ohsugi, J. Phys. Soc. Jpn. **64**, 3656 (1995).
[61] T. Kobayashi, S. Wada, Y. Kitaoka, K. Asayama, and K. Amaya, J. Phys. Soc. Jpn. **58**, 779 (1989).
[62] D.E. MacLaughlin, J.D. Williamson, and J. Butterworth, Phys. Rev. B **4**, 60 (1971).
[63] C. Panagopoulos, J.L. Tallon, B.D. Rainford, T. Xiang, J.R. Cooper, and C.A. Scott, Phys. Rev. B **66**, 064501 (2002).
[64] H. Harashina, S. Shamoto, T. Kiyokura, M. Sato, K. Kakurai, and G. Shirane, J. Phys. Soc. Jpn. **62**, 4009 (1993).
[65] Y. Sidis, P. Bourges, B. Hennion, L.P. Regnault, R. Villeneuve, G. Collin, and J.-F. Marucco, Phys. Rev. B **53**, 6811 (1996).
[66] H. Kohno, H. Fukuyama, and M. Sigrist, J. Phys. Soc. Jpn. **68**, 1500 (1999).
[67] Y. Ohashi, J. Phys. Soc. Jpn. **69**, 2977 (2000).